

# A Barrier Penetration Model for DNA Double Strand Separation

Ajit Kumar Mohanty

*Nuclear Physics Division,*

*Bhabha Atomic Research Centre, Mumbai-400085, India*

## Abstract

A barrier penetration model has been proposed to explain the temperature driven spontaneous melting of the DNA oligomers into two separate single strands whereas the fraction of partially melted intermediate states can be understood on the basis of bound state solution of the effective potential obtained using Peyrard-Bishop formalism. The excellent agreement of the predictions with the recent experimental measurements (Euro. Phys. Lett. 62, 452, 2003, Phy. Rev. Lett. 91, 148101, 2003) provides strong justification for the proposed model. A simple relation has been obtained that correlates the strand stiffness with the temperature at which the spontaneous melting probability becomes half. This is an important outcome as the stiffness parameter of the double stranded conformation can be directly estimated by knowing the mid point temperature which can be measured experimentally. Further, it is shown that the derivative of this probability with respect to temperature is quite sensitive to the parameters of the entropic barrier and can be used as the experimental probes to study the stacking interaction in detail.

PACS numbers:87.10.+e, 03.40.Kf, 05.90.+m

Typeset using REVTeX

## I. INTRODUCTION

The DNA molecule is a double-stranded biopolymer with two complementary sugar-phosphate chains (backbones) twisted around each other forming a right handed helix [1,2]. Each chain is a linear polynucleotide consisting of four kinds of bases: Adenine, Guanine (purines) and Cytosine, Thymine (pyrimidines). The two chains are joined together by hydrogen bonds between pairs of nucleotides, A-T with two hydrogen bonds and G-C with three hydrogen bonds. At sufficiently high temperature, the double stranded DNA (dsDNA) helix melts and the molecules separate into two single strands (ssDNA). The experimental procedure consists in preparing a set of dsDNA with the same length and sequences, which are immersed in an aqueous solution with given physiological conditions. Then the fraction of broken base pairs as a function of temperature, referred to as the melting curve, is measured by the *UV* light absorption, typically at about 260 *nm*. Long DNA molecules give rise to steps in the melting curves corresponding to different regions melting at different temperatures whereas synthetic oligonucleotides do not show any multistep behavior (see [3] for a review). This denaturation process, often interpreted as a reminiscent of a discontinuous first order phase transition, has attracted a great deal of interest to study the physics of highly nonlinear biomolecular system and also it has led to several micromanipulation experiments [4–27]. From biophysics point of view, the strand separation is a key aspect of DNA transcription and replication [28]. During transcription, a transient bubble of ssDNA is formed to allow the enzyme that makes a RNA copy of the DNA sequence to access the DNA bases. During replication that occurs during cell division for example, the dsDNA separates into two, each strand then serving as a template for the synthesis of a new dsDNA. On the otherhand, accurate prediction of DNAs thermal denaturation is an important parameter for many biological techniques like polymerases chain reaction (PCR) where dsDNA are routinely converted to separated ssDNAs by melting at elevated temperature. Therefore, the study of DNA denaturation which is an important biological phenomena has become a subject of interdisciplinary interest.

The early theoretical models like Poland-Scheraga (PS) type [4,29,30] considers the DNA molecule as being composed of an alternating sequence of bound and denaturated (loop or bubble) states. Typically, a bound state is energetically favored over an unbound one while a denaturated segment is entropically favored over a bound one. The DNA denaturation can be viewed as a competition between the entropy of the denaturated loops and the bound state energy of the sequence. In PS type models, the segments that compose the chain are assumed to be noninteracting with each other. This assumption considerably simplifies the calculation of free energy. In the past, the entropy of the denaturated loops has been evaluated by modeling them either as ideal random walks [29] or as self avoiding walks [30]. It has been found that within this approach the denaturation transition of DNA is continuous both in two and three dimensions, and it becomes first order only for  $d \geq 4$ . A denaturated segment in between two bounded structures may introduce flexibility, allowing neighboring segments to interact with the bubble and with each other. Inclusion of this excluded volume interaction effect in PS model drives the transition first order even for  $d = 2$  (and above) [15,16,23,27]. In a different approach, Peyrard and Bishop (PB) [5] proposed a microscopic model to describe the dynamics of the DNA denaturation by introducing an interaction potential which depends on the transverse stretching of the hydrogen bonds between the complementary base pairs. An improved version of this PB model with more realistic treatment of the backbone stiffness [6,7] yields what appears to be a first order phase transition. Despite the simple formalism, the PB model has successfully reproduced the essential features of thermally induced denaturation of long DNA chains. It has been used to estimate the melting curves of very short heterogeneous DNA segments, in excellent quantitative agreement with experimental data [11]. It also provides the characteristic multistep melting behavior observed in heterogeneous DNA sequence [9]. Recently, this model has been used to investigate charge transport properties in DNA chain [31] and the role of nonlinearity and entropy provided by the local base pairs on the interaction of the DNA transcription [32].

As mentioned before, the UV absorption of the spectroscopic measurements are interpreted as the yield for the average fraction of the open base pairs. The denaturation process

leads to a sharp transition from dsDNA to ssDNA when the sequence is long. For short oligomers, this transition is not sharp enough. Due to finite size effect, two fractions, fully dissociated molecules ( $p$ ) due to opening of all the base pairs spontaneously and partially melted intermediate states ( $\sigma$ ), may co-exist over a wide range of temperature below the melting point. From the spectroscopic measurements, it is not possible to estimate these two fractions separately. Recently, a new method has been proposed [33] to quantify the presence of intermediate states and fully open molecules by combining the UV spectroscopy with the quenching technique. The sequences which are partially self-complementary are prepared in the duplex form by hybridizing with the exact reverse complement. On heating, the duplex either melts spontaneously into two separate single strands or remains as connected but with many broken base pairs. Molecules which are completely open form hairpins on quenching while the molecules which are partially open close again as duplexes. The relative amount of hairpins give the fraction  $p$  of completely open molecules whereas the UV spectroscopic measurements yield the fraction of total open base pairs  $f$ . The difference  $\sigma = f - p$  represents the fraction of partially melted intermediate states. This method has yielded new data on the fraction of  $f$ ,  $p$  and  $\sigma$  and also the relative average bubble size  $\langle l \rangle$  as a function of temperatures in the melting transition of several DNA oligomers [33,34]. In this work, we try to understand this new and exciting experimental data both qualitatively and quantitatively within the frame work of PB formalism which has been quite successful elsewhere. We avoid the rigorous solution of the transfer integral (TI) equation to evaluate the configurational partition function. Instead, we concentrate on yet simple but well approximated TI integral which yields a Schrodinger like second order differential equation. For simplicity, we use Morse potential [35] with inclusion of anharmonic stacking interaction [6]. We propose here that for the spontaneous melting of the dsDNA leading to a complete strand separation, the molecules are required to overcome an effective barrier through thermally assisted tunneling whereas the fraction of partially melted intermediate states can be explained on the basis of the bound state solution of the effective potential in the temperature range for which the bound state exists. The excellent agreement of this

prediction with experiments [33,34] provides strong justification for the proposed formalism. Since the spontaneous melting probability is considered as the tunneling phenomena, there exists a mid point temperature at which the thermal energy becomes equal to the height of the entropic barrier. This aspect has been utilized further to derive a simple but an important relation between the double strand stiffness parameter and the mid point temperature which can be determined experimentally. It is shown that the height and the width of the derivative of the double strand separation probability with respect to temperature depend strongly on the parameters of the entropic barrier and thus, can be used as the experimental tool to learn more about the nature of the stacking interaction.

## II. FORMALISM

The details of the PB model with various improvements have been described elsewhere [5–8,12,22] and also we have mentioned it briefly in the appendix for completeness. What concerns here in the present study is the partition function of the configurational part given by

$$Z_y = \frac{1}{\alpha^N} \int_{-\infty}^{\infty} \prod_{i=1}^N dy_n e^{-\beta H(y_n, y_{n-1})}, \quad (1)$$

where the constant  $\alpha$  having the dimension of length has been introduced to make  $Z_y$  dimensionless. The potential energy component  $H(y_n, y_{n-1})$  is

$$H(y_n, y_{n-1}) = \sum_n \frac{1}{2} K (y_n - y_{n-1})^2 + D_n [\exp(-a_n y_n) - 1]^2 - D_n. \quad (2)$$

The index  $n$  runs over all the base pairs and  $\sqrt{2}y_n$  is the relative stretching of the hydrogen bond from the equilibrium position of the  $n^{\text{th}}$  base pair. The first term represents

the stacking interaction potential between adjacent base pairs with a  $y$ -dependent stiffness constant  $K$ . The Morse potential (second term) describes the interaction of the base pairs in the two complementary strands. The parameters of the model, the depth  $D_n$  and the spatial range  $a_n$ , distinguish between the A-T and G-C base pairs. The integral Eq.(1) can be evaluated in the thermodynamic limit using the eigen values and eigen functions of a transfer integral (TI) operator [36]

$$\frac{1}{\alpha} \int dy_{n-1} e^{-\beta H(y_n, y_{n-1})} \phi(y_{n-1}) = e^{-\beta \epsilon} \phi(y_n). \quad (3)$$

It yields  $Z_y = \exp(-\beta N \epsilon_0)$  where  $\epsilon_0$  is the lowest eigen value of a Schrodinger type equation

$$-\frac{1}{2\beta^2 K} \frac{\partial^2 \phi(y)}{\partial y^2} + V(y) \phi(y) = (\epsilon + s_0) \phi(y), \quad (4)$$

where

$$s_0 = \epsilon + \frac{1}{2\beta} \ln \left( \frac{2\pi}{\beta K \alpha^2} \right). \quad (5)$$

As expected, the constant  $\alpha$  does not affect the final expression for  $Z_y$  or the free energy per site  $f = -(1/N\beta) \ln(Z_y) = \epsilon_0$ . However, as will be shown later, it is an important and useful parameter of the present formalism which affects the thermal activation energy  $s_0$  and also it is required to make the TI equation (3) dimensionally consistent. It may be mentioned here that the full partition function that contains all the factors including the kinetic terms is dimensionless due to the phase space factor  $h^{2N}$  in the denominator. Therefore, the factor  $\alpha^N$  in (1) can be considered as the part of the phase space distance associated with only the configurational part of the partition function whose value can be fixed by comparing the results with the experimental measurements. The factor  $K$  is assumed of the form  $K = k_0[1 + \rho(y)]$  so that  $K$  decreases from  $k_0(1 + \rho_0)$  to  $k_0$  at large  $y$ . It is now possible

to separate  $s_0$  into two parts: a  $y$ -dependent positive term which gives an entropic barrier when added to the Morse potential and a  $y$ -independent thermal part  $y_{th}$ , although both parts depend on temperature. Accordingly, Eq.(4) can be rearranged to give

$$-\frac{1}{2\beta^2 K} \frac{\partial^2 \phi(y)}{\partial y^2} + V_{eff}(y)\phi(y) = (\epsilon + \epsilon_{th}) \phi(y), \quad (6)$$

where

$$V_{eff}(y) = \left[ D (e^{-ay} - 1)^2 - D \right] + \frac{1}{2\beta} \ln [1 + \rho(y)], \quad (7)$$

and

$$\epsilon_{th} = \frac{1}{2\beta} \ln \left( \frac{2\pi}{\beta k_0 \alpha^2} \right). \quad (8)$$

In the PB model, a  $y$ -dependent stiffness with an exponential form  $\rho = \rho_0 e^{-by}$  was used to reflect the fact that the DNA is significantly more rigid in the double-stranded conformation than when either of the two interacting base pairs is stretched. Although there is no theoretical guideline, a value of  $b = 0.35 \text{ \AA}^{-1}$  was used in [11] to simulate the melting curves of short heterogeneous DNA sequences ( which accounts for total yield  $f$ ). However, in this study, we have felt the need to use a very small value of  $b$  in order to explain the spontaneous melting fraction of the fully dissociated molecules and partially open intermediate states simultaneously for many oligomers. A small value of  $b$  would mean a flat entropic barrier over a large distance. Although it is very much essential for  $\rho$  to decrease from  $\rho_0$  to 0, the rate of decrease is not found fast enough unless the stretching exceeds a particular limit which may be due to the strong backbone support it receives from the neighboring base pairs while in the double stranded conformation.

## FIGURES

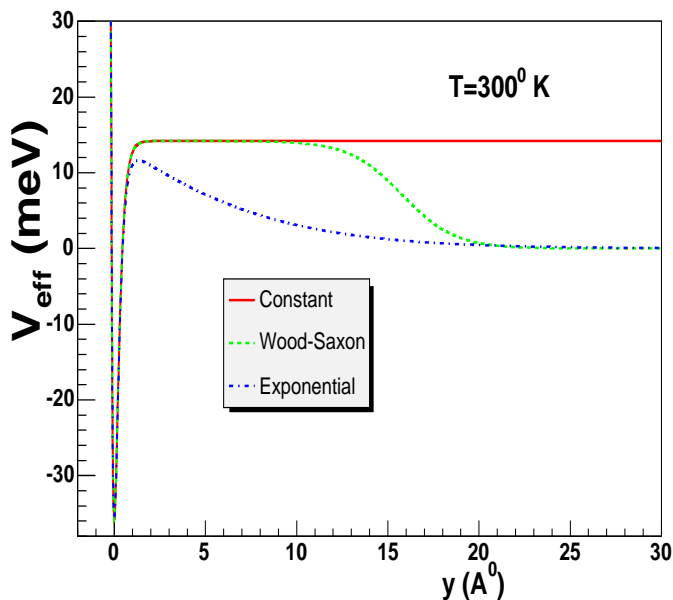


FIG. 1. The effective potential  $V_{eff}$  (in units of meV ) as a function of  $y$ . The parameters are  $D = 0.05$  eV,  $a = 4.2$   $A^{\circ-1}$ ,  $T = 300^0$  K,  $k_0 = 0.013$  eV/ $A^{\circ 2}$  and  $\rho_0 = 2.0$ . For exponential dependence,  $b$  is taken as  $0.2$   $A^{\circ-1}$  whereas for Wood-Saxon form,  $y_0 = 15$   $A^{\circ}$  and  $b = 1.42$   $A^{\circ}$ .

This could be interpreted as some type of co-operative phenomena involving several base pairs with a range larger than what is normally expected. To simulate this effect, we use a slightly different form of Wood-Saxon type

$$\rho = \frac{\rho_0}{1 + e^{-(y-y_0)/b}}, \quad (9)$$

characterized by the depth  $\rho_0$ , range  $y_0$  and diffuseness parameter  $b$ . These are the cooperativity parameters and, in general, may depend on the sequence composition, length of the sequence and also on the buffer conditions. Since it is not known how to fix, these are considered as free parameters to be fixed by the experimental observations. Figure 1 shows a typical plot of the effective potential  $V_{eff}(y)$  as a function of  $y$  at a temperature of  $T = 300^0$ K. The potential parameters are  $D = 0.05$  eV,  $a = 4.2$   $A^{\circ-1}$ ,  $k_0 = 0.013$  eV/ $A^{\circ 2}$  and  $\rho_0 = 2.0$ . For exponential dependence  $b$  is taken as  $0.2$   $A^{\circ-1}$  whereas for Wood-Saxon form,  $y_0$  and  $b$  are chosen as  $15$   $A^{\circ}$  and  $1.42$   $A^{\circ}$  respectively (as an example). The solid



line corresponds to the case when the  $y$ -dependence is ignored. As can be seen from the figure, although both the exponential and the Wood-Saxon forms lead to the same physical consequence, namely, a decrease of the backbone stiffness from  $k_0(1+\rho_0)$  to  $k_0$ , qualitatively, both give rise to two different forms of entropic barriers. We have studied both the forms and prefer to retain the Wood-Saxon form which is found to be more suitable to explain the melting behavior of several oligomers.

### III. DOUBLE STRAND SEPARATION VERSUS INTERMEDIATE STATES

In the following, we describe the method to characterize the fraction of fully open molecules  $p$  and partially melted intermediate states  $\sigma$ . A dsDNA conformation is thermodynamically stable when the free energy per base pair  $\epsilon < 0$ . On the otherhand, for ssDNA,  $\epsilon \geq 0$ . The bound state solution of the Morse potential with the entropic contribution with inclusion of both harmonic and anharmonic stacking interaction has been studied in the past. For long DNA sequence, the denaturation begins with formation of bubbles due to local meltings of different domains (local openings of base pairs) where the base pair bindings are relatively weak. When the average bubble size attains a critical value at temperature close to the melting point ( $T_m$ ), the entropy gain becomes sufficient to overcome the binding and the entire sequence separates into two single strands discontinuously. Therefore, it is only at  $T \gg T_m$ , a real separation is expected. However, for shorter sequences as in the case of many synthetic oligomers, the complete strand separation may occur even below the melting temperature and the melting process may proceed with the co-existence of both fully dissociated molecules ( $p$ ) and partially melted intermediate states ( $\sigma$ ) over a wide range of temperatures [33,34]. It is noticed that the short oligomers ( $< 10$  bp) melt suddenly and the melting curve can be represented by a two state model in which the molecules are either completely closed or completely open. As the oligomer size increases, zipper model seems to be more appropriate which opens continuously giving rise to partially open intermediate states [37]. Many synthetic oligomers which are clamped

at both the ends by the relatively GC rich base pairs may nucleate from the middle AT region continuously until a limiting bubble size is reached after which the melting becomes discontinuous or even depending on the sequence composition, the melting may have contributions from both the processes simultaneously. It is also noticed that the oligomers which are open at one end behave differently than when both the end points are fixed. Therefore, the new experimental measurements with different oligomer designs now impose additional constraints on the theoretical models which are required to explain both  $p$  and  $\sigma$  (hence  $f$ ) simultaneously. Moreover, a quantitative understanding of the melting process of different synthetic oligomers will be a stepforward in gaining more insight of the process by which the base pairs open up locally in a real DNA sequence even at room temperature. In this work, we propose thermally assisted barrier penetration phenomena as a new mechanism for complete strand separation whereas the partially opened intermediate states are interpreted as the bound state solutions of the same effective potential that generates a barrier. These are two distinct processes below the melting temperature although this distinction vanishes as the temperature is raised up to a limit above which the bound state no longer exists. Below the melting temperature, small amplitude coherent fluctuations which involves several base pairs may drive a dsDNA out of the potential well into the continuum for which  $\epsilon \geq 0$ . Although thermodynamically favorable to remain separated, these conformations are still in the dsDNA state (small amplitude fluctuations around the equilibrium value  $y \sim 0$ ) and are required to overcome an entropic barrier (to the right) in order to remain as stable ssDNA conformation. The fraction  $p$ , thus, amounts to calculating the thermally assisted tunneling probability through an entropic barrier with energy  $\epsilon_{th}$  as given by (8) where we have set the free energy  $\epsilon = 0$ . The probability of tunneling can be obtained by solving the Schrodinger Eq.(6) using WKB approximation

$$p = \left(1 + e^{2S}\right)^{-1}, \quad (10)$$

with the action integral

$$S = \int_{y_1}^{y_2} \left[2\beta^2 K(y)\{V_{eff}(y) - \epsilon_{th}\}\right]^{1/2} dy. \quad (11)$$

Note that the term  $1/2\beta^2 K(y)$  is the quantum analog of  $\hbar^2/2\mu$ . When the thermal energy  $\epsilon_{th}$  becomes greater than the barrier height  $V_0$ , the potential barrier can be approximated by an inverted parabola, allowing the use of the analytic expression of Hill and Wheeler [38]

$$p = \left[ 1 + \exp\left\{\frac{2\pi}{\omega}(V_0 - \epsilon_{th})\right\} \right]^{-1}, \quad (12)$$

with

$$\omega = \left[ -\frac{1}{\beta^2 K(y)} \frac{\partial^2 V_{eff}}{\partial y^2} \right]^{1/2}, \quad (13)$$

evaluated at the barrier position  $y_b$ .

Now, using (11) for  $\epsilon < V_0$  and (12) for  $\epsilon \geq V_0$ , the ssDNA fraction  $p$  as a function of  $T$  can be estimated. For the intermediate states, we estimate the quantity

$$\sigma = N \int_{y_{min}}^{y_{max}} |\phi_0(y)|^2 dy, \quad (14)$$

where  $N$  is a normalization constant and  $\phi_0(y)$  is the ground state eigen function of the effective potential  $V_{eff}$  for temperature  $T \leq T_m$ . The integral is bounded by two limits whose values are very crucial to reproduce the experimental observation of the peak to valley ratio of the partially melted intermediate states [34]. In general,  $y_{min} \geq 0$  so that the nucleating bubble gains sufficient entropy to grow whereas  $y_{max}$  defines a range upto which the entropic barrier exists. It may be mentioned here that we do not include the contribution of  $\phi_0(y)$  beyond  $y_{max}$  although  $\phi_0(y)$  is still nonvanishing particularly when  $T$  approaches  $T_m$ . At such high temperature, the ground state energy becomes quite close to the continuum and the melting may proceed with opening of all the remaining base pairs suddenly. Therefore, the fraction of  $\phi_0(y)$  beyond  $y_{max}$  only contributes to the sudden opening which has been already included in Eq.(12) for  $\epsilon_{th} \geq V_0$ . As will be shown later, the experimental data supports a long entropic barrier with range  $y_0 \sim y_{max}$ . Since we are interested for  $\phi_0(y)$  in the range  $y_{min} \leq y \leq y_{max}$ , where the entropic barrier remains practically constant, the ground state solution of the Morse potential with a constant stiffness  $k = k_0(1 + \rho_0)$

$$\phi_0(y) = \sqrt{a} \frac{(2d)^{d-1/2}}{[\Gamma(2d-1)]^{1/2}} \exp(-de^{-ay}) \exp\left[\left(d - \frac{1}{2}\right)ay\right]. \quad (15)$$

can be used to estimate  $\sigma$  (as a good approximation).

It is well known that a sharp melting transition can not be understood only on the basis of the ground state solution of Morse potential with a constant stiffness unless a  $y$ -dependent stacking interaction is included. In the present formalism, the above desired effect is already included in the total yield  $f$  which is now the sum of  $\sigma$  obtained with a constant stiffness as part of the bound state solution and  $p$  which is the tunneling probability through a dynamically generated entropic barrier that includes stiffness variation.

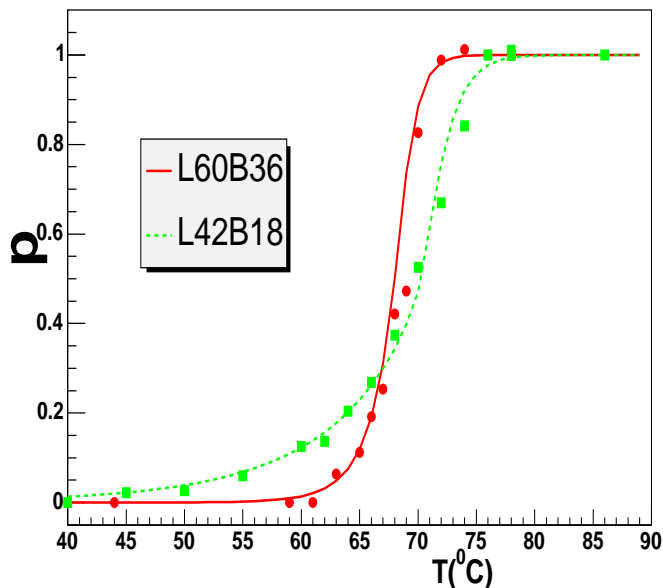


FIG. 2. The fraction of open molecules  $p$  as a function of temperature  $T$  (in  $^{\circ}\text{C}$ ). The parameters are  $D = 0.0494 \text{ eV}$ ,  $a = 4.2 \text{ \AA}^{-1}$ ,  $k_0 = 0.013 \text{ eV/\AA}^2$ ,  $\rho_0 = 1.99$ ,  $y_0 = 40 \text{ \AA}^0$ ,  $b = 4.6 \text{ \AA}^0$  and  $\alpha = 2.18 \text{ \AA}^0$  for *L60B36* sequence and  $D = 0.0505 \text{ eV}$ ,  $a = 4.2 \text{ \AA}^{-1}$ ,  $k_0 = 0.013 \text{ eV/\AA}^2$ ,  $\rho_0 = 2.01$ ,  $y_0 = 15 \text{ \AA}^0$ ,  $b = 1.42 \text{ \AA}^0$  and  $\alpha = 2.18 \text{ \AA}^0$  for *L42B18* sequence. The filled circles and squares are experimental data points

Now using the above formalism, we have estimated both the fraction  $p$  and  $\sigma$  for two synthetic oligomers *L60B36* and *L42B18* which are studied experimentally in ref [34]. Both the oligomers are clamped at the ends with identical GC pairs and with an AT rich middle region of variable lengths (*L60B36*: length  $L= 60$  bases, bubble forming region  $B=36$  bases,

L42B18: L=42 bases, B=18 bases). Figures 2 and 3 show the estimated fractions of completely separated molecules ( $p$ ) and partially melted intermediate states  $\sigma$  as a function of temperature  $T$ . The parameters used in the calculations are listed in the figure captions. The agreement of the theoretical predictions with the experimental measurements is indeed excellent.

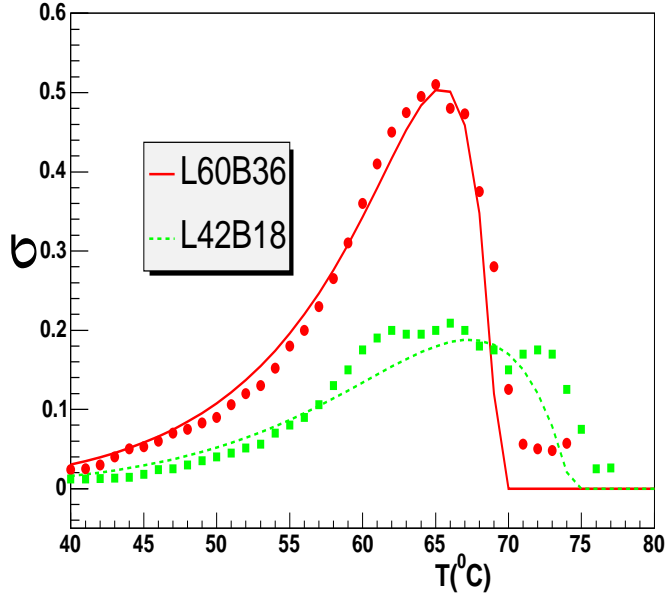


FIG. 3. The quantity  $\sigma = f - p$  as a function of temperature  $T$  (in  $^{\circ}\text{C}$ ). The parameters are  $D = 0.0494 \text{ eV}$ ,  $a = 4.2 \text{ \AA}^{-1}$ ,  $k_0 = 0.013 \text{ eV/\AA}^2$ ,  $\rho_0 = 1.99$ ,  $y_{min} = 9 \text{ \AA}^0$  and  $y_{max} = 40 \text{ \AA}^0$  for *L60B36* sequence and  $D = 0.0505 \text{ eV}$ ,  $a = 4.2 \text{ \AA}^{-1}$ ,  $k_0 = 0.013 \text{ eV/\AA}^2$ ,  $\rho_0 = 2.01$ ,  $y_{min} = 9 \text{ \AA}^0$  and  $y_{max} = 15 \text{ \AA}^0$  for *L42B18* sequence. The normalization constant  $N$  is taken as unity. The filled circles and squares are experimental data points.

Although, initially there are too many free parameters, most of them have been fixed based on different physical considerations. For example, it is noticed that the tunneling probability  $p$  is not very sensitive to the Morse potential as long as they are reasonable, but depends sensitively on the factor  $K(y)$  that decides the nature of the entropic barrier. On the otherhand, the fraction  $\sigma$  and the peak position have strong dependence on the depth and range of the Morse potential. As will be shown later, we fix the Morse parameters that

give optimum fits to the  $\sigma$  measurements. Accordingly, we take  $D = 0.0494 \text{ eV}$  for L60B36 and  $D = 0.0505 \text{ eV}$  for L42B18 whereas  $a$  is fixed at  $4.2 \text{ \AA}^{-1}$  for both the sequences. In fact, these values are nearly identical to what has been used in [11,32] corresponding to an AT base pair. As  $p$  is the tunneling probability, there exists a temperature  $T_d$  at which the thermal activated energy  $\epsilon_{th}$  becomes equal to the barrier height  $V_0$  (tunneling probability becomes 0.5). Since the contribution of the Morse potential is negligible outside the well, it is basically the flat portion of the stacking interaction  $1/(2\beta)\ln(1 + \rho_0)$  that decides the height of the entropic barrier. Equating  $\epsilon_{th}$  with  $V_0$  at  $T_d$  and using the approximation  $V_0 \approx \ln(1 + \rho_0)/(2\beta)$ , we get

$$T_d = \frac{\alpha^2 k_0 (1 + \rho_0)}{2\pi k_\beta}. \quad (16)$$

Thus, the above relation puts the constraint on the choice of  $k = k_0(1 + \rho_0)$  and  $\alpha$ . For same  $T_d$ , we may have different combinations of  $k$  and  $\alpha$ . In practice,  $k$  is really not a free parameter which can be varied randomly as it also controls the temperature dependent effective mass that appears in Eq.(6). Although, we have tried various combinations, it is found that the fit is optimum when  $\alpha$  is close to  $2\text{\AA}$ . This is an interesting observation as this distance also corresponds to an average stretching beyond which the hydrogen bonds start breaking. As we have discussed before,  $\alpha$  is a phase space factor associated with the configurational partition function. It is probably meaningful to expect  $\alpha$  of the order of  $2\text{\AA}$  for the configurational changes to occur. Subsequently, we fix  $\alpha$  at  $2.18\text{\AA}$  which is an optimum choice for all the sequences. With  $\alpha$  fixed, Eq.(16) now gives a very simple but an important relation which can be used to estimate the stiffness parameter  $k = k_0(1 + \rho_0)$  directly by knowing  $T_d$  which can be measured experimentally. For example, from the experimental curves, we estimate  $T_d \sim 68.1^\circ\text{C}$  for L60B36 and  $T_d \sim 70.36^\circ\text{C}$  for L42B18. With the choice of  $\alpha = 2.18\text{\AA}$ , we get  $k \sim 0.0389 \text{ eV/\AA}^2$  and  $k \sim 0.391 \text{ eV/\AA}^2$  for the above two sequences. Although, knowing the full stiffness  $k$  is itself important, yet we do not know how to split it between  $k_0$  and  $\rho_0$ . However, taking the guidance from ref [11] where  $\rho_0$  was taken  $\sim 2$ , we find  $k_0$  should be  $\sim 0.013 \text{ eV/\AA}^2$ . Subsequently, we fix  $k_0$  at

0.013  $eV/A^2$  for all the sequences and consider the co-operative parameter  $\rho_0$  as a variable which, although should be close to 2, can be used as tuning parameter so as to reproduce the correct mid point temperature  $T_d$ . Thus, with  $D$ ,  $a$ ,  $\alpha$ ,  $k_0$  and  $\rho_0$  fixed, we are now left with only two free parameters  $y_0$  and  $b$  which are finally adjusted to reproduce the experimental measurements. As listed in the figure captions, the strength  $\rho_0$  turns out to be 1.99 for L60B36 whereas it is 2.01 for L42B18. This slight variation is expected as both the sequences have different dissociation temperature  $T_d$ . Similarly, the range and diffuseness parameters are found to be  $40A^\circ$  and  $4.6A^\circ$  for L60B36 sequence. The corresponding values for L42B18 are  $15A^\circ$  and  $1.42A^\circ$  respectively. Although it is difficult to draw any definite conclusion, the length  $y_0$  seems to depend strongly on the size of the bubble forming AT rich region or more precisely on the ratio  $B/L$  which are 0.6 and 0.43 respectively for the above two oligomers. It may be mentioned here that this observation is more meaningful for these two oligomers which have identical endpoints and may not be valid in general. However, all sequences studied in this work have a nearly flat entropic barrier over a larger range. This effect, probably, can be interpreted as the reminiscent of a long range co-operative phenomena.

The parameters for  $\sigma$  are also fixed in a similar way. Since the entropic barrier turns out to be nearly constant up to the range  $y_0$ ,  $\sigma$  has been estimated using Eq.(14) with the ground state wave function given by Eq.(15). It is noticed that the peak position of the yield is very sensitive to the melting temperature  $T_m = 2\sqrt{2kD}/(k_\beta a)$ <sup>1</sup>. For a given  $k$  which is fixed from the  $p$  yield,  $\sqrt{D}/a$  ratio (the  $p$  yield is not sensitive to this ratio), is adjusted to have the correct peak position whereas the limit of integrations  $y_{min}$  and  $y_{max}$  are adjusted to reproduce the observed peak to valley ratio. As discussed before, we take  $a = 4.2 A^{\circ-1}$  as

---

<sup>1</sup>Note the distinction between  $T_d$  and  $T_m$  where  $T_d$  is the dissociation temperature at which  $p$  becomes half whereas  $T_m$  is the melting temperature above which the bound state vanishes. In general,  $T_d$  and  $T_m$  need not coincide.

in [11] and use  $D = 0.0494 \text{ eV}$  for L60B36 and  $D = 0.0505 \text{ eV}$  for L42B18 to reproduce the  $\sigma$  curves. It is also noticed that the optimum results are obtained when  $y_{max} \sim y_0$ , i.e. the range of the entropic barrier. Subsequently, we set  $y_{max} = y_0$  and adjust  $y_{min}$  which turns out to be  $9A^\circ$  for both the sequences. Therefore, by putting the constraint to explain both  $p$  and  $\sigma$  measurements simultaneously, we have fixed most of the free parameters of the model. Although,  $y_{min}$  is expected to be  $\geq 0$ , a value of  $9A^\circ$  is indeed too large as compared to the minimum threshold of average stretching  $\langle y \rangle = 2A^\circ$  above which hydrogen bond between the base pairs starts breaking. This large value of  $y_{min}$  probably is very specific to these two oligomers whose end points are fixed by a relatively stronger GC rich regions. An unzipping transition leading to the continuous melting may begin with a nucleating bubble initiating from the softer AT rich middle region. Since this melting is a competition between the energy of the bound states and the entropy of the dissociated states, the transition may not proceed until the bubble radius attains a minimum value which is about  $9A^\circ$  for these oligomers. A stretching distance of  $y_{min} \sim 9A^\circ$  would mean a nucleating bubble of diameter  $d \sim 18A^\circ$  containing about 4 to 5 open base pairs. Unless the size attains this minimum value, the entropy gain is not sufficient enough for the bubble to grow. Note that this minimum size is different from the critical bubble size which is required to drive a spontaneous transition. The  $y_{min}$  value strongly depends on the size and composition of the sequence. We have found that  $y_{min}$  value is much smaller if the sequence is homogeneous. Since the bubble forming AT region of L60B36 and L42B18 oligomers are bounded by relatively stronger GC rich regions at the end, the denaturated bubble may encounter higher resistance to grow due to strong binding. This is to say that the interaction of the bubble with itself and also with its surroundings may bring a reduction in entropy. Therefore, for a given entropy gain, the minimum bubble size required to grow (by compensating the binding energy) for the sequence with fixed end points is larger than the case when the sequence is open at both the ends. This could be viewed as analogous to the excluded volume interaction whose effect is to reduce the entropy of the loop. Notice that when  $y_{min}$  is large or the range  $(y_{max} - y_{min})$  is small, the  $\sigma$  contribution decreases. Another parameter which may also suppress  $\sigma$  yield



is the strong binding effect of the base pair. If the binding energy is large, i.e. if the  $\sqrt{D}/a$  ratio is large, the temperature  $T_m$  at which the bound state vanishes goes up where as the dissociation temperature  $T_d$  remains unaffected. If  $T_d \gg T_m$ , complete dissociation may take place much earlier, thus reducing the fraction of continuous melting. Therefore, in either case, the most probable route available for denaturation is the sudden melting thus making the transition to appear discontinuous.

It may be mentioned here that for a complete strand separation, it is not necessary to raise the temperature until all the base pairs break. Normally, the nucleation is initiated with a small denaturing bubble from the softer AT rich region. When the average bubble size attains a critical value, the loop entropy becomes sufficient enough to overcome the binding so that rest of the base pairs unwind instantly. The critical sized bubble is formed either through a sequential unzipping process what is known as a continuous melting or through the sudden opening due to coherent fluctuation (followed by tunneling). In the first approach, the critical size is reached when the temperature is close to the melting point whereas the second process can happen at any temperature with different probabilities. Since the tunneling probability  $p$  depends only on the entropic barrier parameters, the heterogeneity of the sequence which introduces a site dependent binding  $V_n$ , does not affect the full dissociation yield. On the otherhand, the fraction of the continuous yield  $\sigma$  is strongly affected by the heterogeneity of the sequence. By design, the bubble formation for L60B36 and L42B18 is initiated in the AT rich middle region. Since the AT rich region for L60B36 is long enough, the critical bubble size may still remain confined to the homogeneous middle portion only. For L42B18, the homogeneous AT region may not be long enough and the bubble may extend upto the GC rich region also. As a consequence,  $\sigma$  transition may encounter different melting regions with appropriate weights. As can be seen, the  $\sigma$  peak for L60B36 is more sharper as compared to the case of L42B18 sequence where the GC region may start contributing. This curve can be better understood as a weighted sum over two melting regions with appropriate weights although  $p$  curve can still be understood as a single

tunneling phenomenon through an appropriate entropic barrier.

Figures 4 and 5 show the comparison of  $f$ ,  $p$  and  $\sigma$  with the corresponding experimental results using the set of parameters as listed in the figure captions 2 and 3. The linear rise of the total open base pairs  $f$  after the sigmoidal transition is a well-known phenomenon attributed to the residual base unstacking in the single strands.

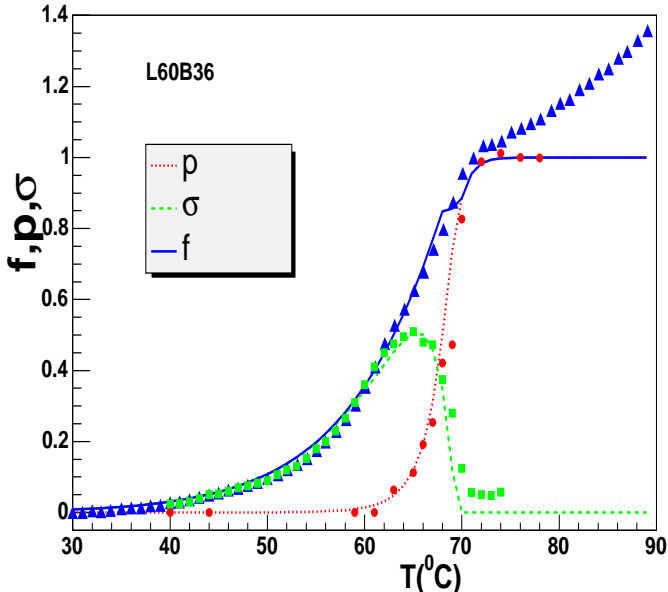


FIG. 4. The quantities  $f$ ,  $p$  and  $\sigma$  as a function of temperature  $T$  (in  $^{\circ}C$ ) for  $L60B36$  sequence. The filled triangles, circles and squares are the corresponding experimental data points.

However, the theoretical prediction of  $f$  does not increase beyond unity as this effect has not been included in the present model.

As shown in figures (2-5), the present model has been quite successful in explaining both qualitatively and quantitatively experimental observations. We have also studied two more oligomers  $L42V1$  and  $L48AS$  for which experimental data points are available [37]. The  $L42V1$  sequence is 42 base pairs long with 18 AT base pairs in the middle whereas  $L48AS$  is 48 base pairs long with a AT rich region of 21 base pairs which is open at one end.

Figure 6 shows the plot of  $p$  as a function of  $T$  for the above two oligomers with the parameters listed in the figure captions. The  $y_0$  parameter is found out to be  $18 A^{\circ}$  for  $L42V1$

with a diffuseness value of  $2.2 A^\circ$ . This oligomer (a  $B/L$  ratio of  $\sim 0.42$ ) is quite identical to L42B18 oligomer in design. Accordingly, the parameters of  $\rho(y)$  follows the systematic and also the full dissociation probability is quite close to that of L42B18 oligomer.

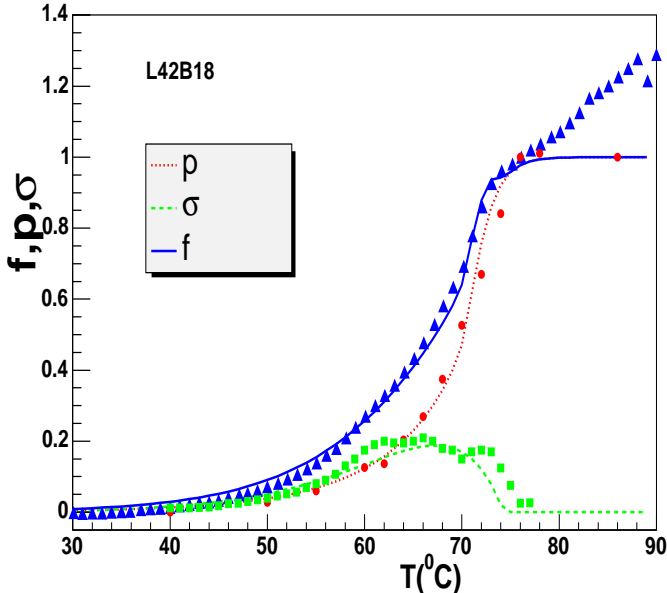


FIG. 5. The quantities  $f$ ,  $p$  and  $\sigma$  as a function of temperature  $T$  (in  $^\circ C$ ) for L42B18 sequence. The filled triangles, circles and squares are the corresponding experimental data points.

Interestingly, this oligomer has no contribution to  $\sigma$  as it melts suddenly at all temperatures. As mentioned before, the vanishing of  $\sigma$  component would mean a vanishing range ( $y_{max} - y_{min}$ ) or a higher effective binding energy which pushes the melting temperature  $T_m$  to the higher side. Since L42V1 is quite similar to L42B18 in design, it is difficult to understand why  $\sigma$  vanishes for the former whereas this component is still significant for the later oligomer. Although this needs more careful analyses, a possible reason could be different buffer conditions in which the DNA solutions were prepared. It is known that a stronger ionic concentration may increase the binding (higher  $D$ , hence higher  $T_m$ ) while the entropic parameters may still remain unchanged. On the otherhand, the melting behavior of L48AS is quite different from the rest of the oligomers as it opens from one end. It has a range which is relatively larger ( $y_0 \sim 60 A^\circ$  and  $b = 9 A^\circ$ ). The large entropic range explains

why  $p$  component is small with a relatively larger  $\sigma$  contribution. We have not estimated the  $\sigma$  fraction, but it is expected to be broad with contributions coming from two different melting regions.

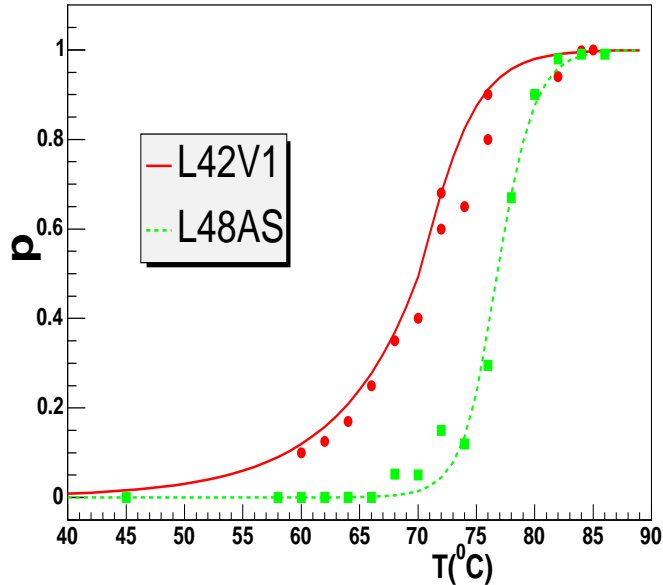


FIG. 6. The fraction of open molecules  $p$  as a function of temperature  $T$  (in  $^{\circ}C$ ). The parameters are  $D = 0.0505$  eV,  $a = 4.2$   $A^{\circ-1}$ ,  $k_0 = 0.013$  eV/ $A^{\circ 2}$ ,  $\rho_0 = 2.01$ ,  $y_0 = 18$   $A^0$ ,  $b = 2.2$   $A^0$  and  $\alpha = 2.18$   $A^{\circ}$  for *L42V1* sequence and  $D = 0.0505$  eV,  $a = 4.2$   $A^{\circ-1}$ ,  $k_0 = 0.013$  eV/ $A^{\circ 2}$ ,  $\rho_0 = 2.07$ ,  $y_0 = 60$   $A^0$ ,  $b = 9$   $A^0$  and  $\alpha = 2.18$   $A^{\circ}$  for *L48AS* sequence. The filled circles and squares are experimental data points

The temperature driven denaturation has also been studied for synthetic ploy (A)- ploy (T) oligomers of various lengths in different buffer conditions [37]. These oligomers can be regarded as homogeneous duplexes held together by identical base pair interaction at the different sites. Although, the measurements do not separate the fractions into fully dissociated and partially open components, the total fraction  $f$  is itself interesting as it has a large not so well understood premelting region. The peak and width of the derivative with respect to temperature also show strong dependence on the length of the oligomer as well as on the buffer conditions. Due to finite size effects, the co-existence of both the components

is expected for these oligomers also. Since data is not available, we will not try to estimate  $p$  and  $\sigma$  exactly so as to reproduce the total yields, rather we will discuss a scenario based on which the experimental results can be understood at least qualitatively. Again as before, we consider an arbitrary oligomer which may have similar potential parameters like L60B36 oligomer except for the fact that this oligomer is now homogeneous. A homogeneous sequence may have a lower  $y_{min}$  value than when the sequence composition is more heterogeneous.

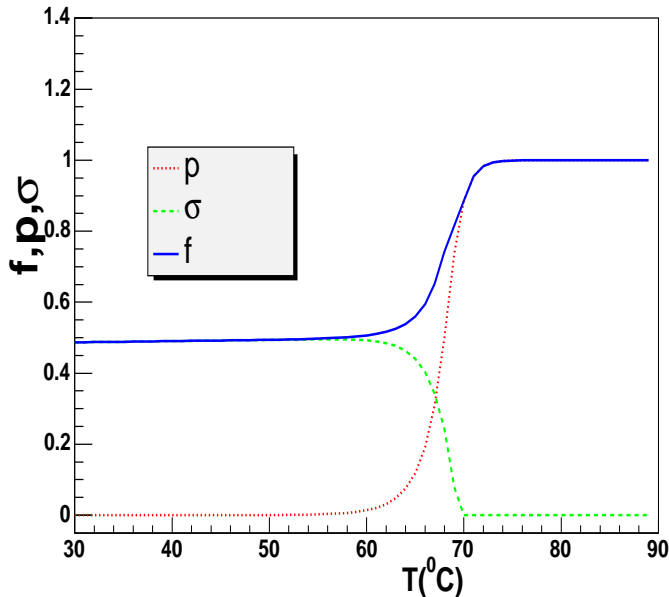


FIG. 7. The quantities  $f$ ,  $p$  and  $\sigma$  as a function of temperature  $T$  (in  $^{\circ}C$ ) for an arbitrary sequence. The parameters are  $D = 0.0494$  eV,  $a = 4.2$   $A^{\circ-1}$ ,  $k_0 = 0.013$  eV/ $A^{\circ 2}$ ,  $\rho_0 = 1.99$ ,  $y_0 = 40$   $A^{\circ}$ ,  $b = 4.6$   $A^{\circ}$ ,  $\alpha = 2.18$   $A^{\circ}$ ,  $y_{min} = 0$ ,  $y_{max} = y_0$  and  $N = 0.5$ .

As a model study, we choose  $y_{min} = 0$ , i.e. the minimum expected value. As the  $y_{min}$  decreases, the behavior of  $\sigma$  changes completely, becoming more uniform as  $y_{min}$  decreases from a higher threshold value towards 0. Figure 7 shows a typical plots of  $\sigma$ ,  $p$  and  $f$  as a function of  $T$  where we have set  $y_{min}$  to its lowest value. Although we have used a normalization factor  $N = 0.5$ , it can be adjusted so as to reproduce the appropriate yield in the premelting region. The total yield is quite similar (at least qualitatively) to what one observes experimentally [37]. Interestingly, the so called premelting region is probably

due to a continuous transition which has nearly uniform probability up to temperature  $T_m$  above which the transition becomes discontinuous. Since below  $T_m$ , the continuous process dominates, a zipper type model may be found more appropriate to describe this type of melting curve, particularly when the sequence is homogeneous and also relatively large. It is also observed that the length of the entropic range  $y_0$  depends on the length of the sequence, i.e. for the same composition,  $y_0$  increases with the length of the sequence probably until an upper limit is reached. So the smaller sequence will have short ranged entropic barrier with increased  $p$  contribution. When the size is very short ( $< 10$  bp), it may completely dissociate without any intermediate state. This explain why a two step model is found more appropriate to describe the melting behavior of very short oligomers.

Since the premelting region is flat, the non vanishing part of the derivative of the total yield is basically due to the fraction  $p$ . Figure 8 shows the plot of  $dp/dT$  (estimated numerically) as a function of  $T$  for different co-operativity parameters. The curves on then left correspond to the case when  $\rho_0 = 1.8$  whereas the curves on the right are for  $\rho_0 = 1.99$ . On both the sides, the solid curve corresponds to the parameters as listed in the figure captions while the dotted and dashed curves are obtained when either  $y_0$  or  $b$  is changed. The point which needs to be stressed here is that the peak positions (hence the temperature  $T_d$ ) are quite sensitive to the strength  $\rho_0$  which may be small for smaller oligomers. Therefore, the shift in peak positions of the oligomers to the higher values when the length increases can be understood on the basis of the increase of the  $\rho_0$  parameter. On the otherhand, the width and the height are very sensitive to  $y_0$  and  $b$  parameters which also depend on the length of the oligomers as well as on the buffer conditions. Therefore, with suitable  $\rho_0$ ,  $y_0$  and  $b$  parameters, it is possible to understand all aspects of the melting behavior of the synthetic oligomers studied in [37].

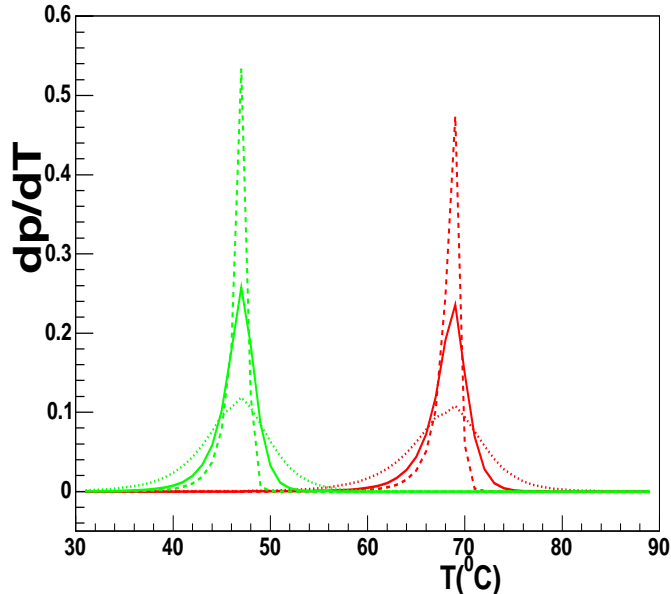


FIG. 8. The derivative of  $p$  as a function of temperature  $T$  (in  $^{\circ}C$ ) for some arbitrary sequence. The parameters are  $D = 0.0494$  eV,  $a = 4.2$   $A^{\circ-1}$ ,  $k_0 = 0.013$  eV/ $A^{\circ 2}$ ,  $\alpha = 2.18$   $A^{\circ}$ ,  $y_0 = 40$   $A^{\circ}$  and  $b = 4.6$   $A^{\circ}$ . The curves on the left correspond to a  $\rho_0$  value of 1.8 whereas the curves on the right are for  $\rho_0 = 1.99$ . In both sets of curves, the solid lines correspond to the parameters as listed above. The dotted lines are obtained when only  $y_0$  is changed from 40  $A^{\circ}$  to 32  $A^{\circ}$  and the dashed lines are obtained when  $b$  is changed from 4.6  $A^{\circ}$  to 3.5  $A^{\circ}$ .

#### IV. CONCLUSIONS

Based on the above studies, we have several conclusions to make. Recall again, a large DNA sequence melts with the initiation of the nucleating bubbles at different regions which are relatively soft. A complete strand separation occurs when the average bubble size attains a critical value. Depending on the nature of the entropic barrier, the domain melting occurs either through continuous opening of base pairs or due to coherent fluctuation followed by tunneling. However, at this level, whatever may be the process of domain melting, the complete dissociation of the full sequence will not be realized unless the average bubble size attains a limiting value so that the entropic gain becomes sufficient to overcome the bound

state energy. Once the melting point is reached, a complete strand separation occurs what appears as a discontinuous phase transition. Therefore, the complete DNA denaturation in the thermodynamic limit can be interpreted as a first order phase transition characterized by a sharp melting temperature at which the bound state vanishes. However, due to finite size effect as in the case of oligomers, both type of processes, one due to continuous opening and the other due to the sudden melting, may co-exist and the concept of a phase transition is not strictly applicable. Therefore, we invoke a barrier penetration phenomena along with the bound state solution to explain these two fractions separately. Although, it is not possible to draw any definite conclusions unless more experimental data sets of various synthetic oligomers are available with different design, we can only make a few qualitative remarks as follows. The available measurements seem to support a long ranged entropic barrier with parameters which depend on the length and composition of the sequence. For the same length, the range of the sequence made up of GC base pairs is higher than when the sequence is homogeneous with AT base pairs. Consequently, the GC rich sequence will have less  $p$  and more  $\sigma$  contributions as compared to the AT rich sequence. If the oligomer is short enough ( $< 10$  bp) and homogeneous, a sudden melting may occur due to an entropic barrier which is very short ranged (small value of  $y_0$ ). These oligomers will also not have any continuous fraction due to vanishing ( $y_{max} - y_{min}$ ) range and the full melting process can be explained by the so called two state model. On the otherhand, with increasing size of the oligomers, the entropic barrier range increases (due to stronger collectivity) and the full dissociation probability  $p$  decreases. If  $y_{min}$  is close to zero, continuous opening takes place with equal probability at all temperatures until the melting point is reached. As seen in [37], these type of processes are characterized by a slowly rising pre-melting region followed by a sudden transition and are more suitable to be described by the zipper type model as contrast to the two state phenomena. The melting behavior of the oligomers studied in [34] can also be understood as the sum of two components. These two oligomers L60B36 and L42B18 with the  $B/L$  ratios of 0.6 and 0.43 are clamped at both the ends with identical GC rich regions. Since the relative AT length is large enough, the bubble forming



region is homogeneous and the corresponding  $y_0$  values of  $40A^0$  and  $15A^0$  are probably following the  $B/L$  (relative length) systematic. The L60B36 has a longer entropic barrier than L42B18 and the corresponding fraction  $p$  is also less for L60B36. On the otherhand, the entropic range is smaller for L42B18. Accordingly, the  $\sigma$  contribution is also less as compared to L60B36. However, the key aspect where these two oligomers differ from not being homogeneous is the higher  $y_{min}$  value of about  $9A^0$  which makes the peak to valley ratio in the  $\sigma$  yield very distinct. The oligomer L42V1 which is nearly identical to L42B18 has also been studied in [33]. While this oligomer has a comparable  $p$  yield, it does not have any  $\sigma$  component. This aspect is interesting and needs further investigations. On the otherhand, the oligomer L48AS has a  $B/L$  ratio of 0.25 with more GC components and also with a large entropic range. Consequently, the  $p$  component for this type of oligomer is negligible and the transition mostly proceeds through continuous opening. For the same reason, as remarked in [34], even shorter oligomer (down to 19 bp) which unzips from one end may open continuously.

Finally, we would like to add here that the shape of the intermediate fraction yield  $\sigma$  depends strongly on the sequence heterogeneity since  $V_n$  becomes site dependent. However, the full dissociation probability  $p$  is still can be obtained from the barrier penetration formalism as it is sensitive only to the entropic barrier. The temperature at which the full dissociation probability becomes half is directly related to the DNA stiffness parameter. For the sequence for which  $T_d = T_m$ , the mid point of the full absorption curve  $f$  can be used to estimate the stiffness parameter. In general,  $T_d$  need not be same as  $T_m$ . Since  $T_d$  relates directly to the stiffness parameter and also its derivative is more sensitive to the parameters of the entropic barrier, it will be more meaningful to study these two components  $p$  and  $\sigma$  separately.

## ACKNOWLEDGMENTS

We would like to thank Prof. Giovanni Zocchi and Yan Zeng for providing the tabulated values of the experimental data points.

## APPENDIX: A

A linear chain of DNA molecules can be described by the Hamiltonian given by

$$H = \sum_n \frac{1}{2} m (\dot{u}_n^2 + \dot{v}_n^2) + \frac{1}{2} K [(u_n - u_{n-1})^2 + (v_n - v_{n-1})^2] + V(u_n - v_n), \quad (\text{A1})$$

where  $u_n$  and  $v_n$  correspond to the displacements of the bases at site  $n$  along the direction of the hydrogen bond, and  $V$  is the potential between the base pairs which can be of the Morse type

$$V(u_n - v_n) = D [\exp\{-A(u_n - v_n)\} - 1]^2. \quad (\text{A2})$$

In terms of the variables  $x_n = (u_n + v_n)/\sqrt{2}$  and  $y_n = (u_n - v_n)/\sqrt{2}$ , the above Hamiltonian can be written as

$$H = \sum_n \left\{ \frac{p_n^2}{2m} + \frac{q_n^2}{2m} \right\} + H(x_n, x_{n-1}) + H(y_n, y_{n-1}), \quad (\text{A3})$$

where  $p_n = m\dot{x}_n$  and  $q_n = m\dot{y}_n$  are the canonical momenta, and

$$H(x_n, x_{n-1}) = \sum_n \frac{1}{2} K (x_n - x_{n-1})^2, \quad (\text{A4})$$

$$H(y_n, y_{n-1}) = \sum_n \left\{ \frac{1}{2} K (y_n - y_{n-1})^2 + D [\exp(-A\sqrt{2}y_n) - 1]^2 \right\}. \quad (\text{A5})$$

The statistical mechanics of the model is described by the partition function

$$Z = \frac{1}{h^{2N}} \int_{-\infty}^{\infty} \prod_{i=1}^N dx_n dy_n dp_n dq_n e^{-\beta H(p_n, x_n, q_n, y_n)}, \quad (\text{A6})$$

where  $\beta = 1/(k_\beta T)$  with  $k_\beta$  being Boltzmann's constant, and  $h$  is Plank's constant. The integrals for the variables  $p_n$ ,  $q_n$ , and  $x_n$  are of the Gaussian type, and give, respectively

$$Z_p = Z_q = (2\pi m k_\beta T)^{N/2}, \quad Z_x = (2\pi k_\beta T/K)^{N/2}. \quad (\text{A7})$$

The remaining configurational partition function  $Z_y$  involves nonlinear Morse potential, and given by

$$Z_y = \frac{1}{\alpha^N} \int_{-\infty}^{\infty} \prod_{i=1}^N dy_n e^{-\beta H(y_n, y_{n-1})}. \quad (\text{A8})$$

The factor  $\alpha$  (dimension of length) has been introduced to make  $Z_y$  dimensionless. The above integral can be evaluated by using the transfer integral (TI) method defined by

$$\frac{1}{\alpha} \int dy_{n-1} e^{-\beta H(y_n, y_{n-1})} \phi(y_{n-1}) = e^{-\beta \epsilon} \phi(y_n). \quad (\text{A9})$$

To compute the integral, we consider a finite chain of  $N$  base pairs and chose periodic boundary conditions by demanding that  $y_N = y_0$ . This amounts to adding a fictitious base pair with index 0 which has the same dynamics as base pair  $N$ , with a simultaneous introduction of a factor  $\delta(y_N - y_0)$ . Consequently, Eq.(A8) can be written as

$$Z_y = \frac{1}{\alpha^N} \int \prod_{n=0}^N dy_n \left[ \prod_{n=1}^N e^{-\beta H(y_n, y_{n-1})} \right] \delta(y_N - y_0). \quad (\text{A10})$$

The  $\delta$  function of  $Z_y$  can be expanded on the base of the eigenfunctions of the TI operator as  $\delta(y_N - y_0) = \sum_i \phi_i^*(y_N) \phi_i(y_0)$ . Performing the integrals over  $y_0, y_1, y_2, \dots, y_{N-1}$  successively yields

$$Z_y = \sum_i e^{-\beta N \epsilon_i} \int dy_N |\phi_i(y_N)|^2 = \sum_i e^{-\beta N \epsilon_i}. \quad (\text{A11})$$

In the thermodynamic limit ( $N \rightarrow \infty$ ), the result is dominated by the term having the smallest value of  $\epsilon_i$  which we denote by  $\epsilon_0$ . The free energy per site is therefore

$$f = -\frac{k_\beta T}{N} \ln(Z_y) = \epsilon_0. \quad (\text{A12})$$

More interesting for the study of DNA denaturation is the mean stretching  $\langle y \rangle$  of the hydrogen bonds. It is given by

$$\langle y \rangle = \frac{1}{Z_y} \int \prod_{n=1}^N y e^{-\beta H(y_n, y_{n-1})} dy_n. \quad (\text{A13})$$

The integral can again be calculated with TI method and yields

$$\langle y \rangle = \frac{\sum_{i=1}^N \langle \phi_i(y) | y | \phi_i(y) \rangle e^{-\beta N \epsilon_i}}{\sum_{i=1}^N \langle \phi_i(y) | \phi_i(y) \rangle e^{-\beta N \epsilon_i}}. \quad (\text{A14})$$

Again, in the limit of large  $N$  and considering only the lowest eigen value  $\epsilon_0$ , the average stretching is given by

$$\langle y \rangle = \langle \phi_0(y) | y | \phi_0(y) \rangle = \int |\phi_0(y)|^2 dy, \quad (\text{A15})$$

for the normalized eigenfunction  $\phi_0(y)$ . Note that with the transformation of the coordinates,  $\sqrt{2} \langle y \rangle$  gives the mean stretching of the hydrogen bond between the two opposite base pairs.

The problem is therefore to find the eigenfunctions and eigen values of the TI operator. The calculation can be made analytically in the limit of strong coupling between sites. For large  $K$ , when  $y_n$  differs significantly from  $y_{n-1}$ , the term  $K(y_n - y_{n-1})^2$  grows rapidly, so that the TI is dominated by the value of  $y_{n-1}$  which are close to  $y_n$ . By defining  $y_{n-1} = y_n + z$  and expanding  $\phi(y_n + z)$  in powers of  $z$ , Eq.(A9) can be written as

$$\frac{1}{\alpha} \int_{-\infty}^{\infty} e^{\frac{-\beta}{2} K z^2} \left[ \phi(y) + z \frac{\partial \phi(y)}{\partial y} + \frac{1}{2} z^2 \frac{\partial^2 \phi(y)}{\partial y^2} \right] = e^{-\beta[\epsilon - V(\sqrt{2}y)]} \phi(y), \quad (\text{A16})$$

where the index  $n$  has been dropped. Since the odd term of the Gaussian integral in  $z$  vanishes, the above integral reduces to

$$\sqrt{\frac{2\pi}{\beta K \alpha^2}} \left[ \phi(y) + \frac{1}{2\beta K} \frac{\partial^2 \phi(y)}{\partial y^2} \right] = e^{-\beta[\epsilon - V(\sqrt{2}y)]} \phi(y). \quad (\text{A17})$$

The factor  $\sqrt{\frac{2\pi}{\beta K \alpha^2}}$  can be absorbed in the eigen value by redefining

$$\bar{\epsilon} = \epsilon + \frac{1}{2\beta} \ln \left( \frac{2\pi}{\beta K \alpha^2} \right). \quad (\text{A18})$$

In many practical situations, the relevant magnitude of  $(\epsilon - V) \sim D$ , the depth of the Morse potential. For positive  $y$  (as in the case for stretching), the Morse potential is bounded by  $D$ . If  $\beta D < 1$ , the exponential can be expanded to get Schrodinger type equation

$$-\frac{1}{2\beta^2 K} \frac{\partial^2 \phi(y)}{\partial y^2} + V(y)\phi(y) = \bar{\epsilon} \phi(y), \quad (\text{A19})$$

where

$$V(y) = D [e^{-ay} - 1]^2, \quad a = \sqrt{2}A, \quad (\text{A20})$$

and  $\bar{\epsilon}$  as defined by Eq.(A18).

The above equation has a discrete spectrum when  $d = \sqrt{2KD}/(k_\beta T a) > 1/2$  and the eigenvalues and the normalized eigen functions of the ground state are then

$$\epsilon_0 = \frac{1}{2\beta} \ln \left( \frac{\beta K \alpha^2}{2\pi} \right) + \frac{a}{\beta} \left( \frac{D}{2K} \right)^2 - \frac{a^2}{8\beta^2 K}, \quad (\text{A21})$$

$$\phi_0(y) = \sqrt{a} \frac{(2d)^{d-1/2}}{[\Gamma(2d-1)]^{1/2}} \exp(-de^{-ay}) \exp[-(d - \frac{1}{2})ay]. \quad (\text{A22})$$

## REFERENCES

- [1] W. saenger, *Principles of Nucleic Acid Structure*, Springer, New York, 1984.
- [2] J. D. Watson, N. H. Hopkins, J. W. Roberts, J. A. Steitz, and A. M. Weiner, *Molecular Biology of the Gene*, 4th ed., Benjamin/Cummings, Menlo Park, CA, 1987.
- [3] R. M. Wartell, and A. S. Benight, *Phys. Rep.* **126**, 67 (1985).
- [4] D. Poland, and H. Scheraga, *Theory of Helix-Coil Transition in Biopolymer*, Academic Press, New York, 1970.
- [5] M. Peyrard, and A. R. Bishop, *Phys. Rev. Lett.*, **62**, 2755 (1989).
- [6] Thierry Dauxois, Michel Peyrard, and A. R. Bishop, *Phys. Rev.* **E47**, R44 (1993).
- [7] Thierry Dauxois, and Michel Peyrard, *Phys. Rev.* **E51**, 4027 (1995).
- [8] Yong-li Zhang, Wei-Mou Zheng, Ji-Xing Liu, and Y. Z. Chen, *Phy. ReV.* **E56**, 7100 (1997).
- [9] Dinko Cule, and Terence Hwa, *Phys. Rev. Lett.*, **79**, 2375 (1997).
- [10] U. Bockelmann, B. Essevaz-Roulet, and F. Heslot, *Phys. Rev. Lett.* **22**, 4489 (1997).
- [11] Alessandro Campa, and Andrea Giansanti, *Phys. Rev.* **E58**, 3585 (1998).
- [12] Su-Long Nyeo, and I-Ching Yang, *Mod. Phys. Lett.* **B13**, 859 (1999), **B14**, 313 (2000).
- [13] Simona Cocco, and Remi Monasson, *Phys. Rev. Lett.* **83**, 5178 (1999).
- [14] David K. Lubensky, and David R. Nelson, *Phys. Rev. Lett.* **85**, 1572 (2000).
- [15] Maria Serena Causo, Barbara Coluzzi, and Peter Grassberger, *Phys. Rev.* **E62**, 3958 (2000).
- [16] Yariv Kafri, David Mukamel, and Luca Peliti, *Phys. Rev. Lett.* **85**, 4988 (2000).
- [17] Nikos Theodorakopoulos, Thierry Dauxois, and Michel Peyrard, *Phys. Rev. Lett.* **85**, 6

- (2000).
- [18] Navin Singh, and Yashwant Singh, cond-mat/0105054 (2001), Phys. Rev. **E64**, 042901 (2001).
- [19] Simona Cocco, Remi Monasson, and John F. Marko, Phys. Rev. **E65**, 041907 (2002); Proc. Natl. Acad. Sci, USA, **98**, 8608 (2001).
- [20] Nikos Theodorakopoulos, cond-mat/0210188 (2002).
- [21] David K. Lubensky, and Davis R. Nelson, Phys. Rev. **E65**, 031917 (2002).
- [22] Thierry Dauxois, Nikos Theodorakopoulos, and Michel Peyrard, J. Stat. Phys., **107**, 869 (2002).
- [23] Enrico Carlon, Enzo Orlandini, and Attilio L. Stella, Phys. Rev. Lett. **88**, 198101 (2002).
- [24] Claudia Danilowicz, Vincent W. Coljee, Cedric Bouzigues, David K. Lubensky, David R. Nelson, and Mara Prentiss, Proc. Natl. Acad. Sci, USA, **100**, 1694 (2003).
- [25] O. Resendis-Antonio, L. S. Garcia-Colin, and H. Larralde, Physica **A318**, 435 (2003).
- [26] Pik-Yin Lai, and Zicong Zhou, Physica **A321**, 170 (2003).
- [27] C. Richard, and A. J. Guttmann, cond-mat/0302514 (2003).
- [28] B. Alberts, D. Bray, J. Lewis, M. Raff, K. Roberts, and J. D. Watson, *Molecular Biology of the Cell 3rd ed.*, Garland Press, New York, 1994.
- [29] D. Poland, and A. Scheraga, J. Chem. Phys., **45**, 1456 (1966), **45**, 1464 (1966).
- [30] , M. E. Fisher, J. Chem. Phys., **45**, 1469 (1966).
- [31] S. Komineas, G. Kalosakas, and A. R. Bishop, Phys. Rev. **E65**, 061905 (2002).
- [32] G. Kalosakas, K. O. Rasmussen, A. R. Bishop, C. H. Choi, and A. Osheva, cond-mat/0309157 (2003).

- [33] A. Montrichok, G. Gruner, and G. Zocchi, Euro. Phys. Lett., **62**, 452 (2003).
- [34] Yan Zeng, Awrasa Montrichok, and Giovanni Zocchi, Phys. Rev. Lett., **91**, 148101 (2003).
- [35] P. M. Morse, Phys. Rev. **34**, 57 (1929).
- [36] J. A. Krumhansl, and J. R. Schrieffer, Phys. Rev. **B11**, 3535 (1975).
- [37] G. Zocchi, A. Omerzu, T. Kuriabova, J. Rudnick and G. Gruner, cond-mat/0304567.
- [38] D. L. Hill, and J. A. Wheeler, Phys. Rev. **89**, 1102 (1953).